The Kinetics of Reduction of Dense Synthetic Nickel Oxide in H_2-N_2 and H_2-H_2O Atmospheres

T. HIDAYAT, M.A. RHAMDHANI, E. JAK, and P.C. HAYES

An investigation of the kinetics of reduction of dense synthetic nickel oxide has been carried out in H_2-N_2 and H_2-H_2O mixtures between 500 °C and 1000 °C. The progress of the reduction was followed metallographically by the measurement of the advance of the nickel product layer. The influences of hydrogen partial pressure, hydrogen-steam ratio, and temperature were systematically investigated in both sets of the mixtures. Increasing hydrogen partial pressure under all conditions investigated results in an increase in the reduction rate. In H_2-N_2 mixtures and H_2-H_2O mixtures with low steam content, the initial reduction rate was found to be first order with respect to hydrogen partial pressure. In both sets of mixtures, it was found that the progress of Ni thickness was not a monotonic function of temperature. A minimum rate of advancement of Ni product was observed between 600 °C and 800 °C, depending on the hydrogen partial pressures and reduction time. The change in reduction behavior is shown to be directly linked to changes in Ni product microstructure.

DOI: 10.1007/s11663-008-9212-0

I. INTRODUCTION

GASEOUS hydrogen reduction of solid NiO is one of the processes used to produce nickel metal. Gaseous reduction is used industrially in a number of operations. For example, basic nickel carbonate (BNC) is converted to nickel oxide and subsequently to nickel metal compacts in the nickel refinery at BHP Billiton, Yabulu Refinery, Australia.[1] The basic nickel carbonate is prepared from laterite ores and from nickel hydroxide intermediate product using a modified Caron process. The nickel hydroxide is in turn sourced from pressure acid leaching operations at Ravensthorpe, Western Australia. Hydrogen reduction of nickel oxide particles produced through pyrohydrolysis of chloride solutions is also being undertaken at the Goro nickel plant Noumea.[2] Another application of the gaseous hydrogen reduction of solid NiO can also be found in the preparation of catalysts.[3,4]

In the industrial practice, the reducing mixtures can also contain significant proportions of nitrogen gas and steam. The presence of these gases has the effect of altering the chemical rate and thermodynamic driving force of the reduction process. In order to enable improvements in the design and control of industrial processes to be undertaken, a systematic study has been undertaken to investigate the effects of hydrogen partial pressure, hydrogen-steam ratio, and temperature on the kinetics of NiO reduction.

The overall reaction for gaseous reduction of nickel oxide with hydrogen can be expressed as follows:

$$NiO\,(s) + H_2\,(g) \rightarrow Ni\,(s) + H_2O\,(g) \qquad [1]$$

Although this appears superficially to be a simple reaction, the reduction of nickel oxide by hydrogen is a heterogeneous reaction that involves a number of complex elementary processes, namely, the following:[5,6]

(1) mass transport of reactant and product gases between gas bulk and reacting oxide particle;
(2) chemical reactions between reactant and oxygen atoms of the oxide;
(3) mass transport of reactants and products in the form of gases, atoms, cations, or anions throughout the particle, including diffusion in condensed phases and porous media; and
(4) nucleation and growth of metal product.

The factors influencing the rates of elementary processes and their influence on the overall rate of reduction and morphology are still not completely characterized. The nature of the chemical reaction steps (2) occurring in heterogeneous reactions of this type, and the microstructural changes accompanying them, are not well characterized. Chemical reaction substeps can occur on both oxide and metal surfaces, when used in relation to metal compound reaction the latter commonly being referred to as autocatalytic reduction processes. Some of these issues have been discussed in previous studies and reviews.[7–12]

Many studies have been undertaken on the gaseous reduction of nickel oxide with hydrogen. A range of particle sizes (100 to 12,000 μm) and sample geometries (powder, pellet, and plate) have been used in

T. HIDAYAT, Postgraduate Student, E. JAK, Director, and P.C. HAYES, Xstrata Professor of Metallurgical Engineering, are with the Pyrometallurgy Research Centre, The University of Queensland, Brisbane, QLD 4072, Australia. Contact e-mail: taufiq.hidayat.1982@gmail.com M.A. RHAMDHANI, formerly Postdoctoral Research Fellow, with the Pyrometallurgy Research Centre, The University of Queensland, is Lecturer, the Faculty of Engineering and Industrial Sciences, Swinburne University of Technology, Melbourne, VIC 3122, Australia.

Manuscript submitted May 18, 2008.
Article published online January 6, 2009.

previous studies.[2–4,13–19] The overall progress of nickel oxide reduction in these studies was monitored by various techniques, such as thermogravimetric method, neutron transmission method, and X-ray diffraction technique. Despite the best efforts of these previous workers to avoid mass-transfer limitations in their experimental design and to control/characterize reaction interface geometry, there is clearly no agreement on the intrinsic chemical reaction rates associated with the reduction conditions.[16]

Recognizing that there is a need to obtain this information, an improved experimental technique for the investigation of the kinetics of reduction of dense synthetic NiO in H_2-N_2 and H_2-H_2O atmospheres using platelike samples of known geometry has been developed. This technique was previously used in the investigation of wustite and magnetite reduction.[20,21] The important features of the technique are as follows:

(1) elimination of the gas phase mass-transfer limitation by utilization of very small samples and high linear gas velocities around the sample;
(2) introduction of the small sample directly into the desired reaction conditions, thus, the sample reaches the reaction conditions in a fraction of a second; and
(3) preservation of the morphology developed in the sample during the reduction by rapidly quenching the partially reduced sample directly into liquid nitrogen.

The progress of the reduction of individual samples after reduction for selected reaction times in the present study was monitored by measuring the thickness of nickel metal product. Systematic investigation of the effects of hydrogen partial pressure, hydrogen-steam ratio, and temperature on the overall rate was achieved by undertaking multiple experiments under a range of process conditions. Examination of the product microstructure was also conducted at selected conditions and related to the kinetics of reduction.

II. EXPERIMENTAL

The method used for the preparation of dense synthetic polycrystalline nickel oxide and the reduction experiment has previously been described in detail by the authors.[22] In brief, high purity nickel sheets (99.98 pct Ni, Sigma-Aldrich, NSW, Australia) were oxidized at 1435 °C for 6 days in air. Each of the oxide sheets was cut to obtain dense NiO samples with dimensions of approximately 2 × 2 × 1 mm.

The reductions of the samples were carried out in a specially designed apparatus shown schematically in Figure 1. The reduction apparatus consists of several major units, *i.e.*, gas burner-preheating (hot-box), reduction furnace, and quenching medium. In the thermally insulated hot-box the gases were heated to 300 °C. In the case of reduction in H_2-H_2O mixtures, this chamber was also used to facilitate the reaction between O_2 and excess of H_2. A burner with a platinum heating element was installed inside the hotbox. The platinum heating element was used to ensure continuous

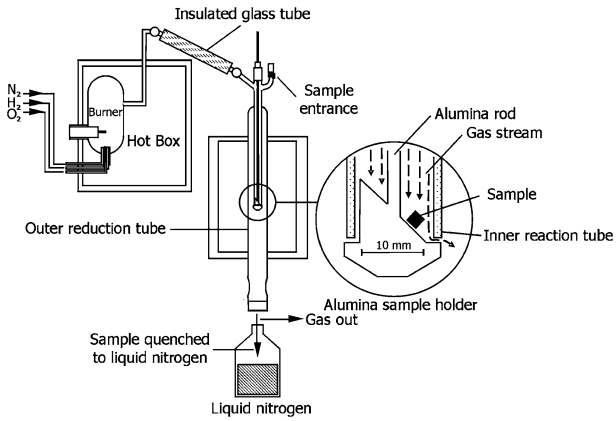

Fig. 1—Arrangement of reduction apparatus.

and complete ignition of H_2 and O_2 gases in the mixing chamber. From this ignition, steam and an excess of hydrogen gas were produced creating selected ratios of H_2-H_2O.

In the reduction furnace the reaction between single dense NiO samples and reducing gas takes place. The sample was directly introduced into the hot-zone of the reduction furnace through an airlock entrance at the top of the apparatus. The sample falls into the reaction tube into a given position on an alumina base attached to an alumina rod. This position is designed to ensure maximum linear gas velocity over the sample surface during the reaction. After the required reduction period the sample was retrieved by lowering the alumina rod. The gap created between the sample holder and the inner reaction tube allows the sample to fall under gravity to the liquid nitrogen quenching medium. The use of liquid nitrogen provides both a thermal quench through cooling of the small sample and a chemical quench by creating a large volume of neutral nitrogen gas around the sample. In this way, the morphology of the sample formed at temperature is retained without change during rapid cooling to room temperature.

By performing reductions using gas mixtures with various H_2-N_2 and H_2-H_2O ratios, the chemical rates and thermodynamic driving forces of the nickel oxide reduction can be independently controlled; the latter is reflected by the difference of oxygen potential between the oxide/metal phase assemblage and the oxygen potential of the gas atmosphere. In the system understudy the activities of nickel and nickel oxide are unity relative to the pure solids. The Gibbs free energy of formation of NiO was taken from the FactSage thermodynamic database version 5.5.[23] The changes to the chemical rate was carried out by varying the proportions of H_2-N_2, while the changes to the thermodynamic driving force was carried out by varying the hydrogen to steam ratio. The flow of each of the gases entering the reduction furnace was controlled by using calibrated pressure differential type flowmeters. A total flow-rate of 1000 mL min^{-1} (1 atm, 25 °C) was applied to minimize the resistance to the gas phase mass transfer from the bulk gas to the outer surface of the particle.

The progress of the reduction reaction was followed by measuring the advance of Ni product layer after selected reaction times on a series of separate samples. To enable these observations, the cross sections of the partially reduced samples were prepared using conventional metallographic technique, *i.e.*, mounting the samples at 90 deg to the major axis in acrylic resin, grinding with silicon carbide paper, and polishing using diamond paste from 6 to 0.25 μm. The observations of the sample cross sections were carried out using optical microscopy OLYMPUS*AX70 and scanning electron microscopy (SEM) under a backscattered electron mode with Philips XL-30 (Philips is currently part of FEI Company, Hillsboro, OR). For selected conditions, investigation of the product structures was also carried out using a cold-field emission gun SEM JEOL** 6400F. For the examination under Philips XL-30 and JEOL 6400F, the samples were first coated with Pt using Eiko IB-5 Sputter Coater (Eiko Co. Ltd., Hitachinaka, Japan) for 5 minutes.

*Olympus is a trademark of Olympus Corp., Tokyo.

**JEOL is a trademark of JEOL Ltd., Tokyo.

A typical example of the observed cross section of a partially reduced NiO sample is shown in Figure 2. The thickness of nickel product, Δx, formed on the outer surface of the sample was measured in each case within a particular NiO grain. By doing so, any uncertainties resulting from preferential reduction of NiO at microcracks or grain boundaries (Figure 3) can be eliminated. The values of nickel product thickness reported here are the mean values measured from samples that were products of two or more replicate experiments. In each sample, the measurements were carried out at three or more different NiO grains.

At low temperatures and low hydrogen partial pressures the nickel product did not develop uniformly as a function of time due to the presence of an induction period associated with the formation of Ni nuclei on the oxide surface. In this case, the measurements were carried out on the largest advance of nickel product, which corresponds to the nucleus that appeared at the earliest reduction time.

In the present study, an accurate measurement of nickel thickness using the present technique can be carried out at times as short as 5 seconds. At times shorter than 5 seconds the accuracy of the experiment can be dependent on the operator of the experiment. If the kinetic information at shorter reaction times and higher reaction rates is required, then other experimental techniques should be considered.

Although uncertainty associated with the preferential reduction and variations in particle geometry has been minimized, there remains a small variation of nickel thickness in the partially reduced NiO grain due to factors such as the shrinkage of the nickel product, deviation from 90 deg in sectioning of the sample, reduction timing, *etc*. Evaluation of the uncertainty due to shrinkage of the nickel product was given particular attention. The method of determining reaction kinetics used in the present study assumes that the thickness of Ni (Δx) resulting from the reduction process is equal to the thickness of original NiO. In practice some differences may be expected due to changes of Ni metal through sintering and volume change during reduction. A special series of experiments was therefore undertaken to measure this uncertainty at different conditions.

Nickel oxide samples were prepared from high purity nickel sheets using the same method as that adopted for the kinetic experiments. The oxidation of the metal sheet results in a cavity (void) at the center of the solid due to the outward diffusion of nickel atoms through the nickel oxide films. By splitting samples into two parts along this cavity, two completely solid samples are obtained from each piece. The surfaces of these new samples are then polished to produce smooth parallel surface. Each of the oxide samples were fractured perpendicular to the solid surface to create a pair of identical samples. One part of the sample was reduced at the most extreme temperature in the present study, *i.e.*, 1000 °C using 100 pct H_2 (1 atm, 250 mL min^{-1}) for 160 seconds, approximately twice the time required for complete reduction of the sample, while the other part was kept as

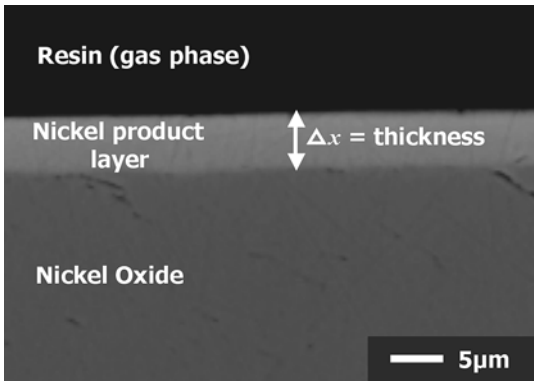

Fig. 2—Example of a polished cross section of a NiO sample partially reduced at 500 °C under 100 pct H_2 (1 atm).

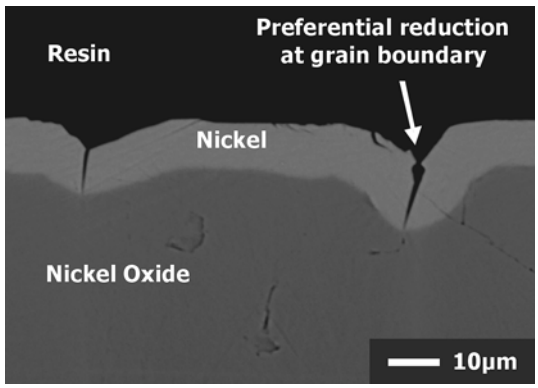

Fig. 3—Example of preferential reduction at grain boundaries during reduction of dense polycrystalline NiO.

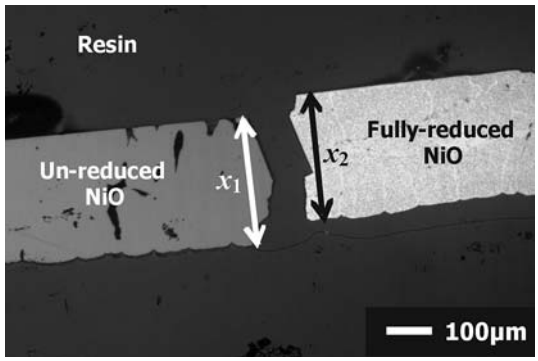

Fig. 4—Example of unreduced and fully reduced oxide sample prepared from identical starting sample (reduction carried out at 1000 °C for 160 s in 100 pct H_2 (1 atm, 250 mL min^{-1})).

the original. The fully reduced and unreduced sample pairs were mounted in acrylic resin and prepared using the metallographic technique described previously (Figure 4). From optical micrographs of the cross sections, measurements of the thickness of the reduced and unreduced samples were obtained.

Tests were undertaken at 1000 °C since it is expected that the maximum sintering or shrinkage will occur at the highest temperature examined in these experiments. It was shown that the average linear shrinkage during the reduction under these conditions is approximately 2.2 pct. This shrinkage value is relatively small compared to uncertainties associated with other factors, such as deviation from 90 deg in sectioning of the sample, reduction timing, *etc*., which are estimated to be less than 10 pct. Therefore, it is reasonable to assume at this stage that the thickness of Ni (Δx) resulting from the reduction process equals the thickness of original NiO.

III. RESULTS

A. *Reduction in H_2-N_2 Atmospheres*

Experiments in H_2-N_2 atmospheres were performed for selected times, temperatures, and H_2-N_2 ratios. The nickel product layer thicknesses resulting from these experiments were measured and the mean value at each condition ($\Delta\bar{x}$) calculated. The experimental conditions and the results of the measurements are provided in Table I. The divergence of results at each set of conditions is presented in terms of standard deviation (σ). A small standard deviation indicates that many data points are close to the mean value, while a high standard deviation indicates scattered data points. In the later subsections, the influence of each variable on the reduction process will be examined.

1. *The progress of NiO reduction with time*

The results of the measurement of Ni product thickness as a function of time during the reduction of dense NiO under various H_2-N_2 compositions and temperatures are shown in Figure 5. The measurements conducted on dense NiO grain reduced at 500 °C at various hydrogen partial pressures (Figure 5(a)) show that, under these conditions, the reaction rates within experimental uncertainty are constant with reaction time. The same trend was also observed in the reduction of NiO at 600 °C in 100 and 75 pct H_2 mixtures (Figure 5(b)). The linear relationship between nickel product thickness and time suggests that the effective reduction condition at the reaction interface, *i.e*., chemical rate and thermodynamic driving force, is not changing throughout the reduction process.

In contrast, a change of reduction rate with time may suggest that there is a change in the effective reduction condition or boundary conditions with time that affected the overall reduction process; this was found to be the case for NiO reduction carried out at temperatures above 600 °C. The change in reduction behavior can be seen clearly in the reduction of NiO at 700 °C, 800 °C, 900 °C, and 1000 °C. For example, Figures 5(c) through (f) show that up to 5 seconds the reduction rates were fast, but as the reaction time progressed slower reduction rates were observed for a given gas mixture and temperature. In the case of the reduction of NiO at 700 °C under 100 pct H_2-1 atm (Figure 5(c)) it was observed that the initial rate was rapid (5.1 μm s^{-1} between 0 to 5 seconds). However, after 50 seconds of reduction the rate decreased to approximately one-tenth of the initial value (*i.e*., 0.57 μm s^{-1}).

2. *Effect of hydrogen partial pressure*

The results of the measurements of Ni product thickness as a function of hydrogen partial pressure are presented in Figure 6. At the shortest time of reduction (5 seconds), there is almost a linear relationship between the Ni product thickness and hydrogen partial pressure, *i.e*., the reaction is first order with respect to the hydrogen partial pressure. For example, at 800 °C and 5 seconds (Figure 6(d)), NiO reduction under hydrogen partial pressure of 0.26 atm resulted in nickel product with thickness of 3.5 μm. The increase of hydrogen partial pressure to 0.53 and 1 atm (approximately two and four times 0.26 atm) increased the nickel thickness to 7.3 and 14.0 μm, respectively (*i.e*., two and four times of the previous value). A similar trend was also observed for the reduction at 900 °C and 1000 °C as shown in Figures 6(e) and (f). At lower temperatures, the linear relationship between nickel thickness and hydrogen partial pressure was even extended to 20 and 40 seconds for NiO reduction carried out at 600 °C and 500 °C, respectively (Figures 6(a) and (b)).

At longer reduction times, there are changes in the relationship between nickel product thickness and hydrogen partial pressure and time. The disappearance of the linear relationship between nickel product thickness and hydrogen partial pressure was evident for all temperatures. For instance in the experiment carried out at 600 °C and 80 seconds (Figure 6(b)), the reduction under hydrogen partial pressure of 0.75 atm produced nickel with thickness of 168.2 μm. The decrease of hydrogen partial pressure to 0.26 atm at the same reaction time rapidly decreased the thickness of nickel

Table I. Measurement of Ni Product Thickness Developed during NiO Reduction in H_2-N_2 Atmospheres (P Total = 1 Atm)*

	Gas Composition ($H_2/H_2 + N_2$)											
	100 Pct H_2			75 Pct H_2			53 Pct H_2			26 Pct H_2		
T (°C)	t (s)	$\Delta\bar{x}$ (μm)	σ	t (s)	$\Delta\bar{x}$ (μm)	σ	t (s)	$\Delta\bar{x}$ (μm)	σ	t (s)	$\Delta\bar{x}$ (μm)	σ
500	5	3.06	0.43	15	6.60	0.76	10	3.04	0.20	20	4.29	0.15
	10	5.98	0.12	20	10.44	0.32	20	6.80	0.11	40	9.28	0.22
	20	12.53	0.18	40	21.79	0.38	40	18.20	0.47	80	22.14	0.19
	40	27.46	0.27	80	42.65	0.43	80	37.32	0.15	—	—	—
	80	52.30	0.83	—	—	—	—	—	—	—	—	—
	120	70.60	1.57	—	—	—	—	—	—	—	—	—
600	5	10.38	0.23	10	17.95	0.74	5	3.58	0.19	10	7.04	0.37
	10	25.49	0.63	20	43.02	0.79	10	11.32	0.58	20	13.57	0.38
	20	56.31	1.05	40	72.76	0.96	20	26.35	0.36	40	15.49	0.24
	40	99.75	2.29	80	168.22	7.20	40	53.63	2.48	80	17.08	0.25
	80	201.69	9.81	—	—	—	80	77.73	3.77	—	—	—
675	5	24.08	0.52	5	13.31	0.30	5	9.84	1.06	5	5.74	0.17
	10	42.41	0.67	—	—	—	—	—	—	—	—	—
	20	57.56	2.12	—	—	—	—	—	—	—	—	—
	40	79.21	2.42	—	—	—	—	—	—	—	—	—
	80	118.59	6.25	—	—	—	—	—	—	—	—	—
700	5	25.70	0.53	5	12.82	0.44	5	8.75	0.33	5	5.31	0.42
	10	36.26	1.11	10	22.56	1.19	10	12.23	0.12	10	9.83	0.26
	20	48.01	0.47	40	28.78	0.68	20	17.94	0.44	20	11.94	0.37
	40	62.21	0.49	40	36.75	0.83	40	27.13	0.19	40	13.16	0.37
	80	84.91	0.95	80	45.28	4.87	80	31.62	0.26	80	14.82	0.80
725	5	18.26	1.68	5	11.95	0.44	5	8.49	0.48	5	3.77	0.13
750	5	17.49	0.64	5	11.13	0.54	5	8.07	0.27	5	3.09	0.17
775	5	15.93	0.39	5	11.14	0.28	5	7.25	0.50	5	3.15	0.22
800	5	14.00	0.51	5	9.72	0.66	5	7.30	0.59	5	3.48	0.46
	10	20.58	0.54	10	18.92	0.61	10	13.45	0.20	10	5.00	0.41
	20	35.67	1.78	20	26.13	1.01	20	19.47	1.16	20	9.04	0.55
	40	54.59	3.38	40	38.03	0.88	40	28.46	2.41	40	12.10	0.13
	80	81.28	1.77	80	52.14	0.08	80	41.15	3.36	80	18.00	0.95
900	5	19.09	0.49	5	11.77	0.36	5	8.84	0.61	5	4.45	0.63
	10	31.08	0.33	10	19.53	0.70	10	16.72	0.23	10	8.64	1.38
	20	51.14	1.53	20	37.96	1.27	20	24.41	1.40	20	14.23	0.65
	40	81.35	1.62	40	57.16	0.67	40	37.79	0.10	40	25.76	1.23
	80	121.89	2.23	80	96.05	2.51	80	69.23	0.78	80	41.29	2.16
1000	5	26.27	1.98	5	17.69	0.52	5	12.27	0.77	5	6.71	0.26
	10	42.08	4.39	10	33.76	0.44	10	25.62	1.71	10	12.31	0.53
	20	79.02	3.22	20	57.14	1.75	20	38.39	1.09	20	22.46	1.79
	40	119.61	2.54	40	91.36	1.69	40	70.48	2.09	40	37.32	0.52
	80	193.21	9.64	80	147.11	7.33	80	107.45	2.65	80	64.09	1.66

*Note: T = temperature, t = time, $\Delta\bar{x}$ = mean product thickness, and σ = standard deviation.

to 17.1 μm. The complexity of the relation between hydrogen partial pressure and nickel product thickness at longer reduction times may be associated with the overall process that is governed by mass-transport processes as a result of thicker product layer, as well as changes in the structure of porous product.

3. *Effect of temperature*

The Ni product thickness as a function of temperature for a given H_2-N_2 mixture during the reduction of dense NiO in H_2-N_2 mixtures is shown in Figure 7. It can be seen that the progress of Ni thickness is not a monotonic function of temperature. It was found that an increase of reduction temperature does not always lead to an increase in the reduction rate. Figure 7(a) shows that reduction carried out at 700 °C for 5 seconds under pure hydrogen (1 atm) produced nickel with thickness of 25.7 μm. Increasing the temperature to 800 °C for the same period of reduction resulted in a nickel product with thickness of only 14.0 μm. The unusual behavior became more marked as the reaction time was increased. For example, after 80 seconds of reduction process the product thickness resulting from reduction at 600 °C was 201.7 μm, whereas nickel product thicknesses of only 80 μm were obtained when reductions were carried out between 700 °C and 800 °C.

The trends in behavior were observed to be a function of bulk gas composition. The rate minimum was observed to become less marked as the gas mixture was changed from 100, 75, 53, to 26 pct hydrogen

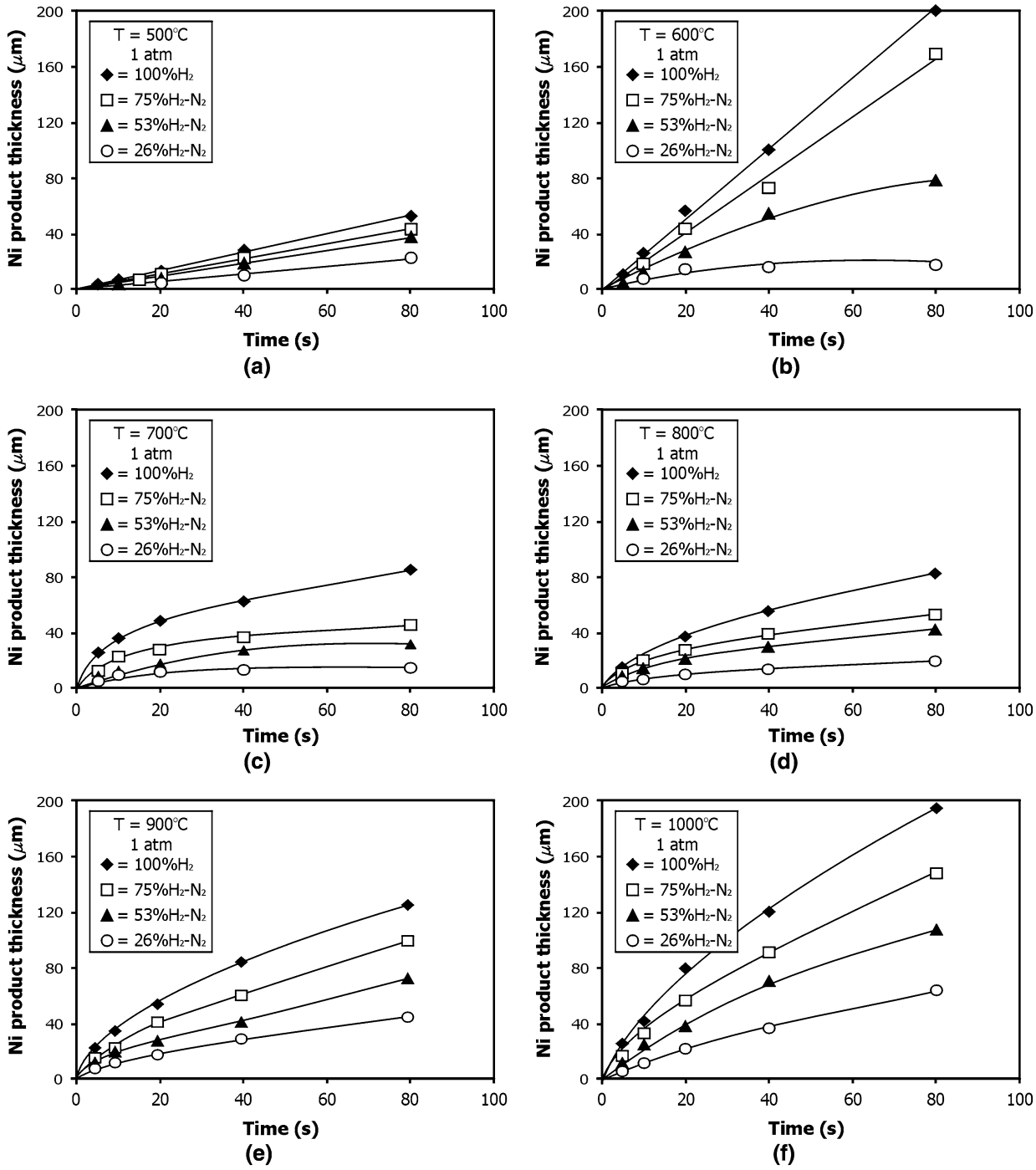

Fig. 5—Measured mean Ni product thicknesses as a function of time during NiO reduction under H_2-N_2 atmospheres at various hydrogen partial pressures (P total = 1 atm) at (*a*) 500 °C, (*b*) 600 °C, (*c*) 700 °C, (*d*) 800 °C, (*e*) 900 °C, and (*f*) 1000 °C.

(Figures 7(a) and (d)). At 26 pct H_2 the product thickness at a given time was relatively unchanged on increasing temperature from 500 °C to approximately 800 °C.

It appears that this anomalous reduction behavior is greatly dependent on the reduction conditions. The hydrogen partial pressure and reduction temperature were found to be the key factors governing the maximum and minimum extent of the nickel product advancement in the range of conditions investigated.

B. *Reduction in H_2-H_2O Atmospheres*

The experimental conditions and the Ni product thickness resulting from the reduction experiments in H_2-H_2O atmospheres are provided in Table II.

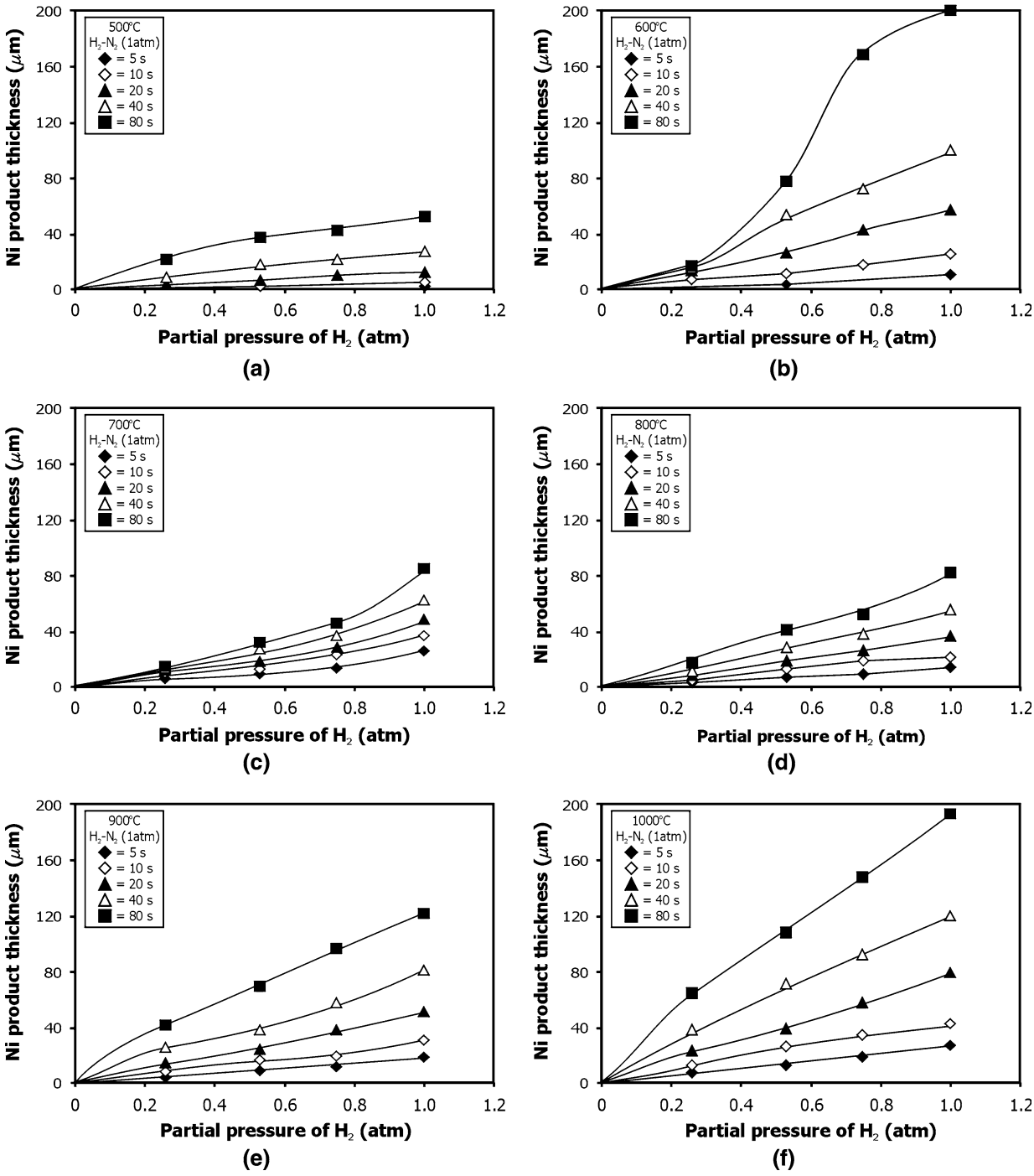

Fig. 6—Measured mean Ni product thicknesses as a function of hydrogen partial pressure (P total = 1 atm) during NiO reduction under H_2-N_2 atmospheres at various times at (*a*) 500 °C, (*b*) 600 °C, (*c*) 700 °C, (*d*) 800 °C, (*e*) 900 °C, and (*f*) 1000 °C.

Further evaluation of the influence of each variable to the reduction process is carried out in subsequent subsections.

1. *Progress of NiO reduction with time*

The results of the measurements of the nickel product thickness as a function of time during the NiO reduction in H_2-H_2O atmospheres are shown in Figure 8. The experiments at 500 °C show that the rates of reduction were constant with time under all gas conditions as shown in Figure 8(a). However, at 600 °C it was found that the reduction rate was independent of reduction time only for H_2-H_2O gas mixtures containing 80 pct H_2 or over (Figure 8(b)).

For temperatures above 600 °C, the progress of reduction with time was found to be nonlinear and decreasing with time. The example of a decrease in reduction rate can be seen in the NiO reduction at 900 °C under 90 pct H_2 (Figure 8(e)). Between 0 and 5 seconds the reduction rate was found to be 3.4 $\mu m \cdot s^{-1}$,

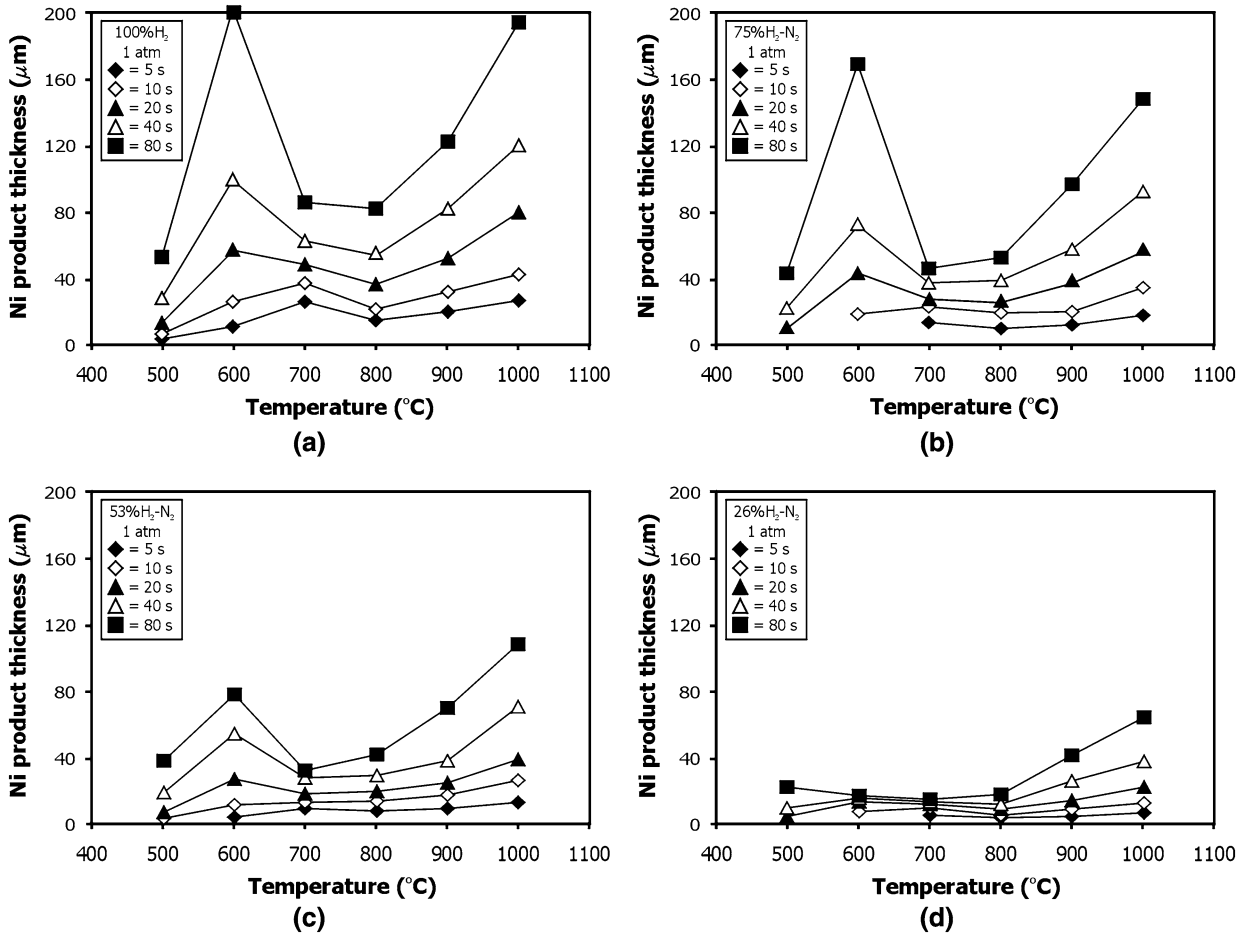

Fig. 7—Measured mean Ni product thicknesses as a function of temperature during NiO reduction under H_2-N_2 atmospheres at various reduction times at (*a*) pH_2 = 1 atm, (*b*) pH_2 = 0.75 atm, (*c*) pH_2 = 0.53 atm, and (*d*) pH_2 = 0.26 atm (P total = 1 atm).

while between 20 and 40 seconds the reduction rate decreased to 0.7 $\mu m \cdot s^{-1}$.

2. *Effect of hydrogen partial pressure*

Figure 9 shows the plots of nickel product thickness as a function of hydrogen partial pressure in the NiO reduction under H_2-H_2O mixtures. Below 675 °C a steep nonlinear decrease of the porous nickel product thickness with decreasing of hydrogen partial pressure was observed. At 500 °C and 240 seconds a 30 pct decrease of hydrogen partial pressure from 0.9 to 0.6 atm significantly decreased the nickel product thickness by a factor of 88 pct, from 116.2 to 13.2 μm (Figure 9(a)). At 600 °C and 80 seconds when the hydrogen partial pressure was lowered from 0.9 to 0.6 atm, the nickel thickness also decreased greatly from 195.9 to 38.7 μm.

In the NiO reduction at 800 °C and above, the nickel product thickness appears to decrease linearly with decreasing hydrogen partial pressure. At 800 °C and 80 seconds, the decrease of hydrogen partial pressure from 0.9 to 0.6 atm was accompanied by a 30 pct drop of nickel thickness from 70.1 to 52.3 μm (Figure 9(d)). It may be concluded that the retardation of the reduction process by the presence of steam at high temperatures was less pronounced than that at lower temperatures, and may be associated with different rate-limiting processes.

3. *Effect of temperature*

The effect of temperature on the reduction behavior of NiO in H_2-H_2O mixtures can be seen in Figure 10. Consistently, the minimum thickness for a given reduction time was observed in the range of 675 °C and 800 °C. As the hydrogen partial pressure is decreased the temperature corresponding to the minimum decreases, being approximately 675 °C at 60 pct H_2-H_2O (Figures 10(b) through (d)). The differences between nickel thicknesses at the minimum and those at the adjacent temperatures were not significant at short reduction times, however, as the reduction time increased the differences became more pronounced. Again it appears that the reduction conditions influence the anomalous behavior in NiO reduction.

IV. DISCUSSION

To investigate the actual effect of reaction variables on the NiO reduction, the values of intrinsic reaction rates of reduction should be considered. The intrinsic

Table II. Measurement of Ni Product Thickness Developed during NiO Reduction in H_2-H_2O Atmospheres (P Total = 1 Atm)*

	Gas Composition ($H_2/H_2 + H_2O$)											
	90 pct H_2			80 pct H_2			70 pct H_2			60 pct H_2		
T (°C)	t (s)	$\Delta\bar{x}$ (μm)	σ	t (s)	$\Delta\bar{x}$ (μm)	σ	t (s)	$\Delta\bar{x}$ (μm)	σ	t (s)	$\Delta\bar{x}$ (μm)	σ
500	30	10.62	0.30	60	14.46	1.08	60	8.01	0.65	120	6.10	0.40
	60	27.39	0.84	120	31.65	1.12	120	15.51	0.42	240	13.18	0.79
	120	64.59	1.87	240	76.98	5.97	240	51.09	2.57	—	—	—
	240	116.18	2.23	—	—	—	—	—	—	—	—	—
600	5	8.29	0.22	10	15.18	1.02	10	7.65	0.12	20	9.87	0.35
	10	19.98	2.22	20	30.41	2.30	20	18.50	1.29	40	24.80	0.79
	20	49.10	1.11	40	79.01	0.45	40	55.76	2.48	80	38.69	0.96
	40	96.93	1.74	80	154.94	5.98	80	118.70	4.84	—	—	—
	80	195.88	5.92	—	—	—	—	—	—	—	—	—
675	5	19.84	0.58	10	17.09	0.64	10	9.92	0.33	10	5.38	0.41
	10	32.94	1.48	20	28.18	1.55	20	14.68	0.28	20	8.97	0.39
	20	40.39	0.86	40	38.26	0.73	40	30.99	0.96	40	15.37	0.60
	40	53.30	1.58	80	50.85	1.48	80	45.65	1.48	80	23.69	0.90
	80	65.48	4.43	—	—	—	—	—	—	—	—	—
800	5	12.33	1.13	5	10.24	0.20	10	11.42	0.44	10	6.90	1.17
	10	19.00	0.30	10	16.05	1.05	20	17.13	0.55	20	14.71	1.36
	20	34.88	1.08	20	29.52	1.31	40	37.64	0.09	40	32.94	1.57
	40	49.33	1.08	40	41.50	1.52	80	56.69	1.56	80	52.25	1.08
	80	70.11	2.13	80	61.82	2.15	—	—	—	—	—	—
900	5	16.93	1.53	5	16.08	1.88	5	9.58	0.39	10	14.89	1.04
	10	26.19	2.66	10	23.98	1.28	10	18.36	0.52	20	25.88	0.57
	20	44.54	1.04	20	39.06	1.03	20	32.69	1.05	40	53.13	1.11
	40	67.03	1.91	40	59.48	1.77	40	56.71	1.89	80	86.84	2.13
	80	110.64	1.68	80	104.98	2.17	80	91.93	1.58	—	—	—
1000	5	22.14	1.12	5	22.44	1.95	5	15.36	0.12	5	13.92	0.39
	10	38.14	1.55	10	36.01	1.25	10	28.00	1.00	10	30.13	2.00
	20	61.38	1.05	20	56.80	1.71	20	52.93	1.24	20	47.85	1.47
	40	105.58	4.10	40	91.99	2.93	40	84.65	1.47	40	81.06	1.55
	80	156.97	2.17	80	150.24	2.19	80	132.72	2.07	80	123.07	1.24

*Note: T = temperature, t = time, $\Delta\bar{x}$ = mean product thickness, and σ = standard deviation.

reaction rate referred to in this context is defined as the rate of chemical reactions occurring at the Ni-NiO interface, independent of the influence of gas phase mass transfer through the gas film boundary layer surrounding the particle and through the product layer formed on the particle. The present experiments have been designed to ensure that gas phase mass transfer is not the rate-limiting step of the process. This condition is fulfilled at the initial stage of reduction where the product thickness is low and the diffusive flux of gas through the product layer is high and not rate limiting.

Realizing this fact, the intrinsic reaction rate can be acquired from the initial reaction rate at a particular set of reduction conditions. Assuming that nucleation of Ni metal product is rapid and the outer surface is uniformly and completely covered by nickel in a very short time, the initial reaction rate is considered to be given by the maximum limiting slope of the product thickness *vs* reaction time. In the present study the shortest possible time of experiment with high accuracy is 5 seconds, hence the limiting slopes in all conditions were calculated between 0 and 5 seconds. In the case demonstrated in Figure 11 for NiO reduction at 1000 °C using 100 pct H_2 (1 atm), the initial reaction rate constant was calculated between the zero point (0 seconds, 0 μm) and the first point of the measurement, *i.e.*, (5 seconds, 26.27 μm). The initial reaction rate k obtained from this calculation is 5.25 $\mu m \cdot s^{-1}$.

The values of initial reaction rate of NiO reduction in H_2-N_2 atmospheres are provided in Table III. The plots of the initial reaction rates *vs* hydrogen partial pressure are shown in Figure 12. It can be seen that the initial reaction rates are linearly dependent on the hydrogen partial pressures, *i.e.*, described by a first-order reaction equation (rate = kP_{H_2}) at any given temperature. The linear first-order relationship between initial reaction rates and hydrogen partial pressures was also observed in the study by Rashed and Rao.[16]

For H_2-H_2O mixtures, the values of initial reaction rate of NiO reduction are provided in Table IV and plotted as a function of hydrogen partial pressure in Figure 13. At low steam content a linear relationship between initial reaction rates and hydrogen partial pressure is still observed. The measured reaction rates are the same as observed in H_2-N_2 mixtures of equivalent hydrogen partial pressure. At higher steam

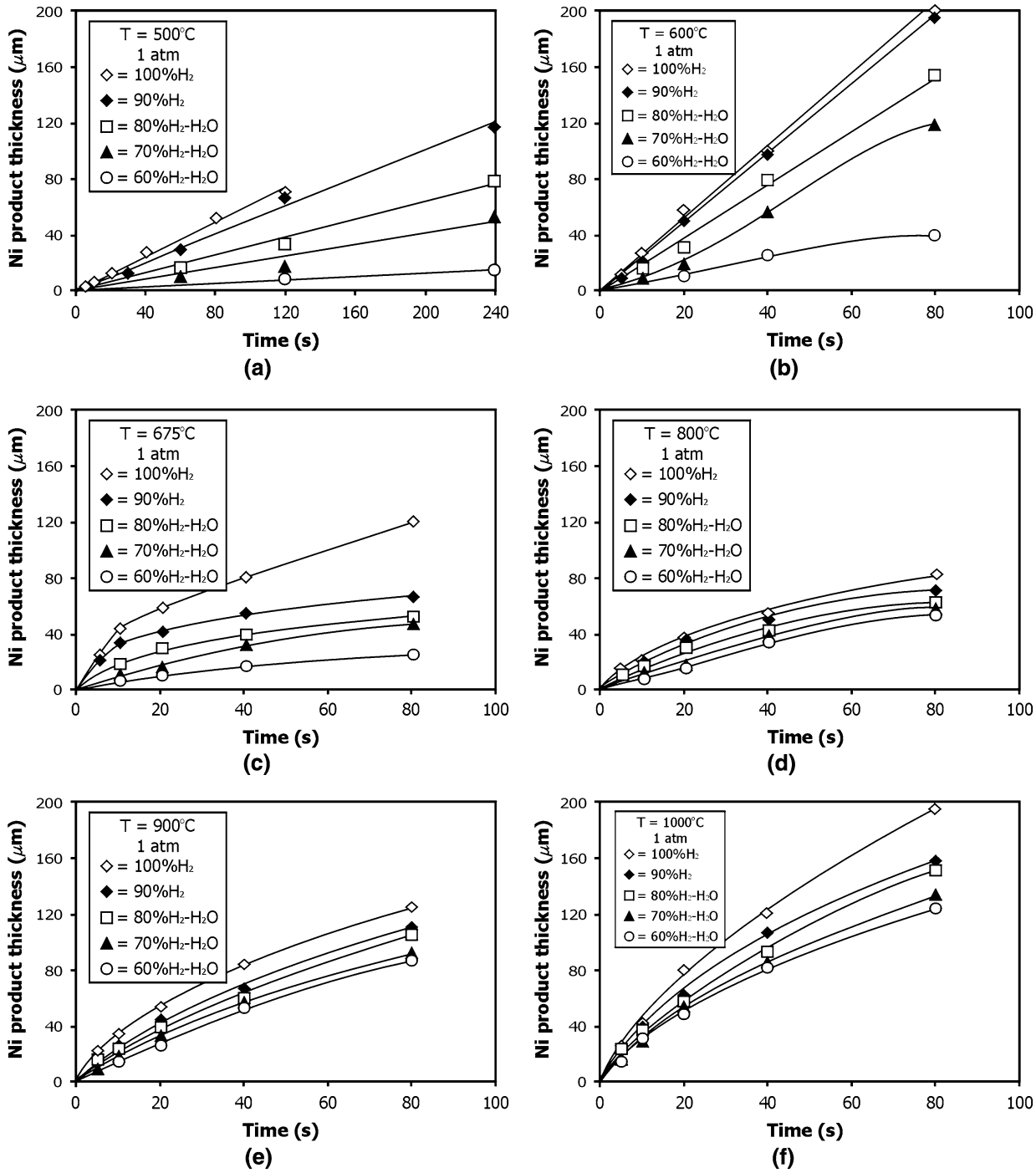

Fig. 8—Measured mean Ni product thicknesses as a function of time during NiO reduction under H_2-H_2O atmospheres at various hydrogen partial pressures (P total = 1 atm) at (*a*) 500 °C, (*b*) 600 °C, (*c*) 675 °C, (*d*) 800 °C, (*e*) 900 °C, and (*f*) 1000 °C.

content, there was no nickel nuclei formed between 0 and 5 seconds. Therefore, the initial reaction rates data at steam content greater than 40 pct is not available, except for temperatures of 1000 °C. It should be noted that even after long reaction times, after metal nucleation and growth has occurred across the entire surface, the rates of nickel oxide reduction at low hydrogen partial pressures are orders of magnitude slower than at high hydrogen partial pressures, the decrease in rate is much greater than can be accounted for by a first-order change in rate with hydrogen pressure. This is a significant observation that has important industrial implications.

These observations appear to be explained by two principal phenomena. In the initial stage of reduction, particularly at low temperatures, the retardation is

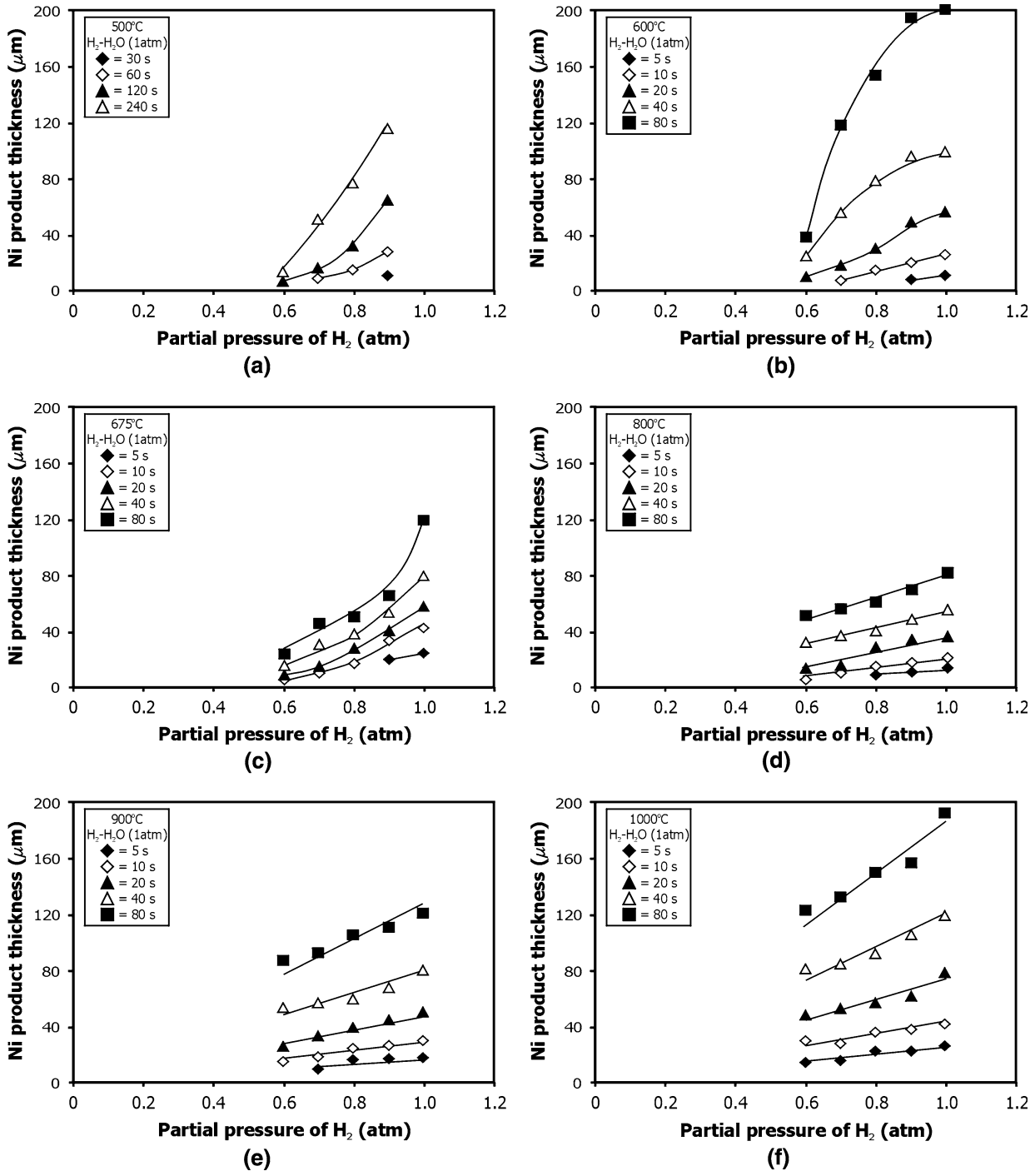

Fig. 9—Measured mean Ni product thicknesses as a function of hydrogen partial pressure (P total = 1 atm) during NiO reduction under H_2-H_2O atmospheres at various times at (*a*) 500 °C, (*b*) 600 °C, (*c*) 675 °C, (*d*) 800 °C, (*e*) 900 °C, and (*f*) 1000 °C.

reflected by the difficulty in forming metal nucleus. In the absence of nickel metal the oxide surface rapidly approaches local equilibrium with the gas phase since the volume diffusion of nickel into the nickel oxide bulk is low. The overall reaction rate at the surface is therefore progressively lowered. The presence of metal nuclei allows the excess nickel in the oxide to precipitate out. In the extreme conditions, as the steam concentration in the gas phase approaches equilibrium with the oxide, the formation of dense metal nucleus covering the surface of the reaction interface.[22] Therefore, it is important to maintain the reduction atmosphere with high hydrogen partial pressure and high hydrogen-steam ratio. By maintaining this condition, a complete removal of oxygen in the NiO reduction process can be achieved.

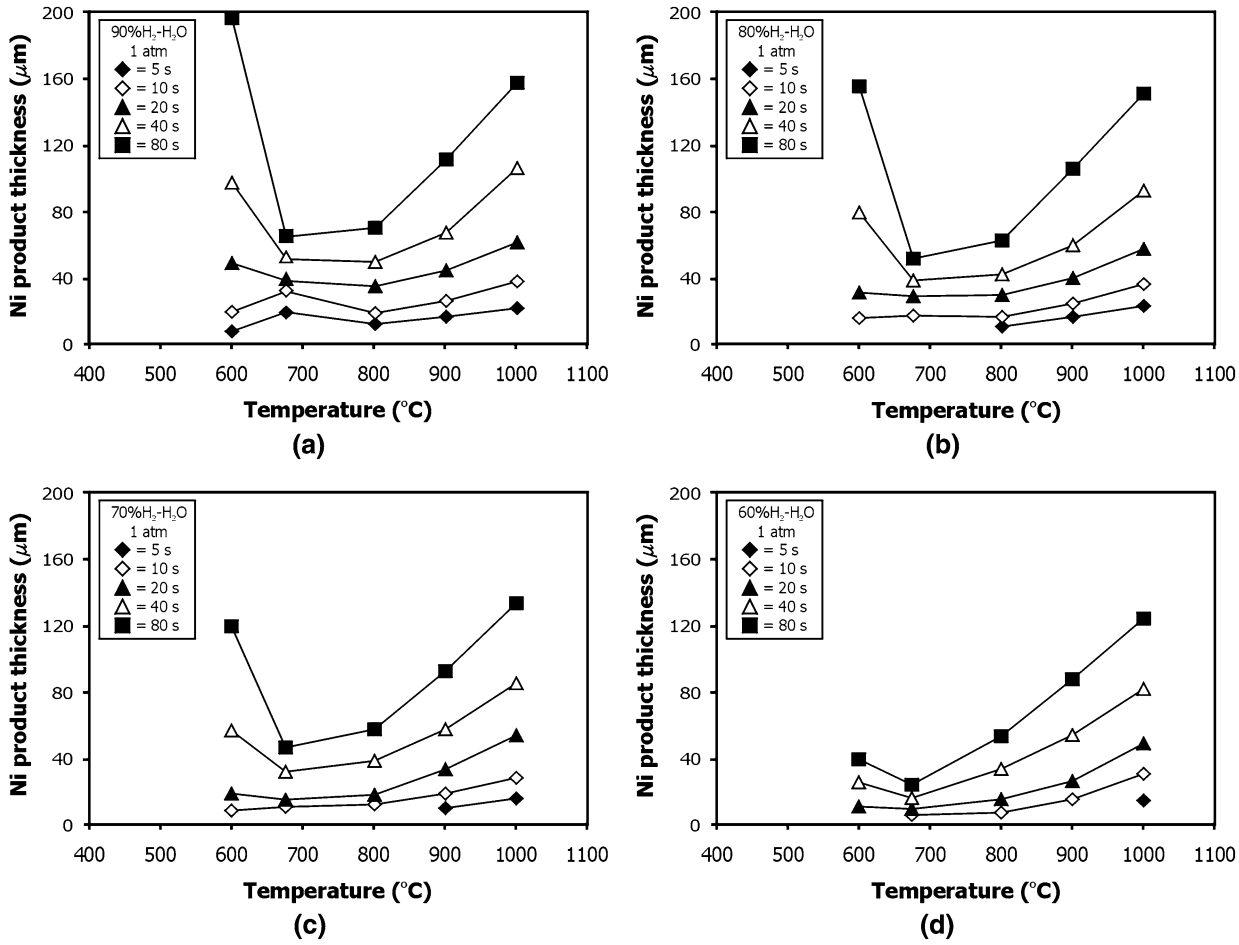

Fig. 10—Measured mean Ni product thicknesses as a function of temperature during NiO reduction under H_2-H_2O atmospheres at various reduction times at (*a*) pH_2 = 0.9 atm, (*b*) pH_2 = 0.8 atm, (*c*) pH_2 = 0.7 atm, and (*d*) pH_2 = 0.6 atm (P total = 1 atm).

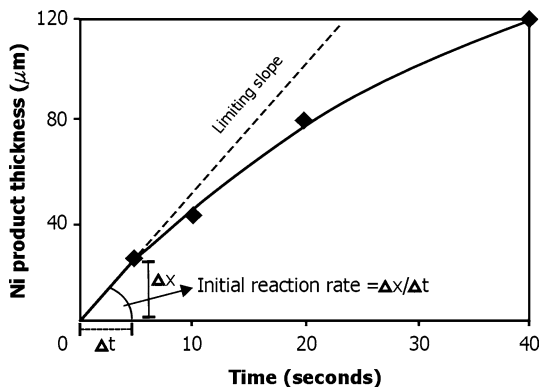

Fig. 11—Example of derivation of initial reaction rate for NiO reduction from the limiting slope of the product thickness *vs* time plot (reduction at 1000 °C in 100 pct H_2, 1 atm).

Arrhenius plots of the rates of NiO reduction of the present and previous results[16,24] at a hydrogen pressure of approximately 1 atm are shown in Figure 14. In the figure, the NiO reduction rates are presented as flux of oxygen removal. The original data of Rashed and Rao[16] were presented in the form of oxygen flux, while the rates of the present study and Pluschkell and Sarma[24] need to be converted from linear Ni product growth rate ($\mu m \cdot s^{-1}$).

The flux of oxygen removal is equal with the flux of NiO consumption by hydrogen gas as shown by the following equation:

$$-J_O = -J_{NiO} = \frac{-k_{NiO}\rho_{NiO}}{M_{NiO}} \quad [2]$$

where J_O is flux of oxygen removal (mol $O \cdot m^{-2}\ s^{-1}$), J_{NiO} is flux of NiO consumption by hydrogen gas (mol $O \cdot m^{-2}\ s^{-1}$), ρ_{NiO} is density of NiO ($g \cdot m^{-3}$), M_{NiO} is molecular weight of NiO ($g \cdot mol^{-1}$), and k_{NiO} is the rate of NiO consumption ($m \cdot s^{-1}$). Assuming that the volume of the reduced NiO is equal to the volume of Ni produced by the reduction, *i.e.*, there is no significant shrinkage or expansion of Ni product layer (average linear shrinkage equals 2.2 pct), the rate of NiO consumption will be equal to the rate of Ni layer advancement.

$$-k_{NiO} = k \quad [3]$$

where k is the rate of Ni layer advancement ($m \cdot s^{-1}$). Initial measurements indicate that this assumption holds over the temperature range and conditions investigated, *i.e.*, 500 °C to 1000 °C, although it has been

Table III. Initial Reaction Rates of NiO Reduction between 0 and 5 Seconds in H_2-N_2 Atmospheres (P Total = 1 Atm)*

	Volume Percent H_2							
	100 Pct		75 Pct		53 Pct		26 Pct	
T (°C)	k (μm·s^{-1})	σ	k (μm·s^{-1})	σ	k (μm·s^{-1})	σ	k (μm·s^{-1})	σ
500	0.61	0.09	—	—	—	—	—	—
600	2.08	0.05	—	—	0.72	0.04	—	—
675	4.04	0.12	2.66	0.06	1.97	0.21	1.15	0.03
800	2.80	0.10	1.94	0.13	1.46	0.12	0.70	0.09
900	3.82	0.10	2.35	0.07	1.77	0.12	0.89	0.13
1000	5.25	0.40	3.54	0.10	2.45	0.15	1.34	0.05

*Note: σ = standard deviation.

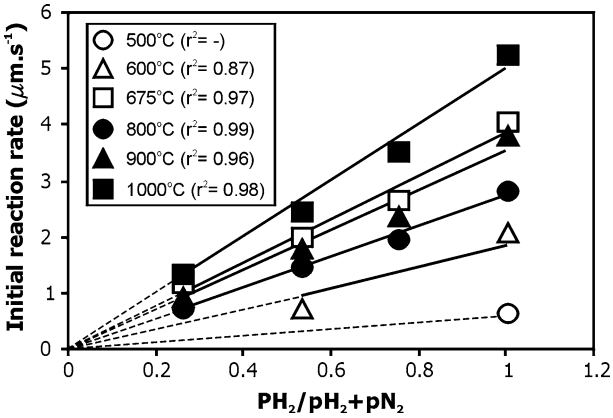

Fig. 12—Effect of hydrogen partial pressures on initial reaction rates of NiO reduction in H_2-N_2 atmospheres obtained between 0 and 5 s (P total = 1 atm).

shown that the changes in product microstructure do occur as reduction proceeds. Hence, the flux of oxygen removal can be calculated from the initial reaction rates obtained by the current work and by Pluschkell and Sarma[24] by the following relation:

$$-J_O = \frac{k\rho_{NiO}}{M_{NiO}} \quad [4]$$

with ρ_{NiO} and M_{NiO} equal to 6.55×10^6 (g m^{-3}) and 74.7 (g mol^{-1}), respectively.

The Arrhenius plot shows that in general the rates increase with temperature. It can be seen that studies carried out by Pluschkell and Sarma[24] and Rashed and Rao[16] are in good agreement (Figure 14). The experimental techniques used by these researchers were designed to eliminate possible effects of gas phase mass-transfer process, *i.e.*, by (1) direct observation and measurement of the radial growth of the nickel metal nuclei on the surface of dense nickel oxide,[24] and (2) measurement of the reduction rates of very thin NiO samples (54-μm thickness) using a thermogravimetric technique.[16]

The initial reaction rate of NiO reduction obtained by the present authors at approximately 500 °C is within 10 pct of the data of Pluschkell and Sarma,[24] having similar activation energy to that observed in the previous studies. The rates measured by Pluschkell and Sarma are slightly greater than those of Rashed and Rao[16] below 400 °C, but there is good agreement between 400 °C and 450 °C.

In the present study it was observed that between 700 °C and 800 °C the reaction rate decreases with the increase of temperature. As the temperature is further increased between 800 °C and 1000 °C, the initial reaction rate again increases, however, the activation is lower than that between 500 °C and 700 °C. The slowdown in reaction rate during NiO reduction has previously been reported.[2,25] However, the overall rates in the previous studies are considerably less than those observed in the present work, indicating a significant

Table IV. Initial Reaction Rates of NiO Reduction between 0 and 5 Seconds in H_2-H_2O Atmospheres (P Total = 1 Atm)*

	Volume Percent H_2									
	100 pct		90 pct		80 pct		70 pct		60 pct	
T (°C)	k (μm·s^{-1})	σ	k (μm·s^{-1})	σ	k (μm·s^{-1})	σ	k (μm·s^{-1})	σ	k (μm·s^{-1})	σ
500	0.61	0.09	—	—	—	—	—	—	—	—
600	2.08	0.05	1.66	0.04	—	—	—	—	—	—
675	4.04	0.12	3.97	0.12	—	—	—	—	—	—
800	2.80	0.10	2.47	0.23	2.05	0.04	—	—	—	—
900	3.82	0.10	3.39	0.31	3.22	0.38	—	—	—	—
1000	5.25	0.40	4.43	0.22	4.49	0.39	3.07	0.02	2.78	0.08

*Note: σ = standard deviation.

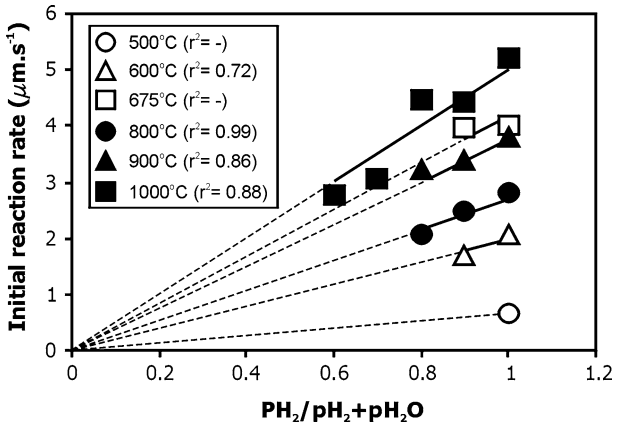

Fig. 13—Effect of hydrogen partial pressures on initial reaction rates of NiO reduction in H_2-H_2O atmospheres obtained between 0 and 5 s (P total = 1 atm).

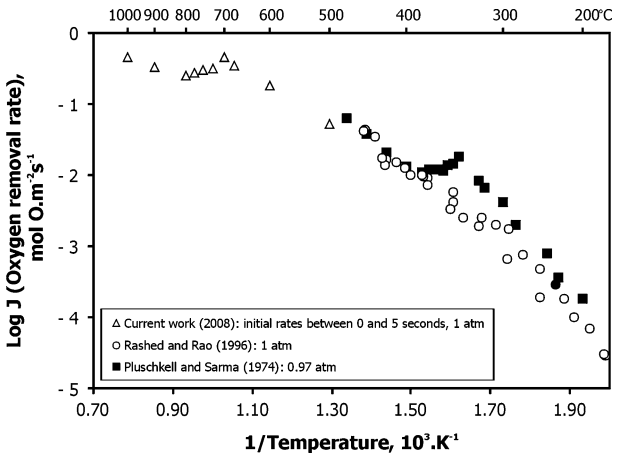

Fig. 14—Arrhenius plot of initial reaction rates of NiO reduction (represented in terms of oxygen removal rate) in H_2-N_2 atmospheres from the present results (P total = 1 atm) and results by Rashed and Rao[16] and Pluschkell and Sarma.[24]

contribution of gas phase mass-transfer processes in the earlier work.

Using the Arrhenius equation

$$k = k_o \exp\left(-\frac{Q}{RT}\right) \quad [5]$$

where k, k_o, R, T, and Q refer to reaction rate at certain temperature, frequency factor, gas constant, temperature, and activation energy, respectively, the apparent activation energies of NiO reduction using 100 pct H_2 (1 atm) observed in the present study can be calculated. At temperatures between 500 °C and 700 °C, the apparent activation energy of the reduction process is 66.6 kJ mol^{-1}, while between 800 °C and 1000 °C, it was found to be 34.8 kJ mol^{-1}. This indicates that as temperature is increased from 700 °C to 800 °C there is a change in rate-limiting reaction mechanism.

To further investigate this anomalous behavior, examination of microstructures was carried out for the products resulting from 5 second reduction of NiO under 100 pct H_2 (1 atm) between 500 °C and 1000 °C. These partially reduced samples were first fractured using a scalpel blade, sputter coated with platinum, and then examined using the SEM (JEOL 6400F). Examples of microstructures found in these selected samples are provided in Figure 15.

It can be seen that as the result of NiO reduction between 500 °C and 700 °C, Ni product microstructures that consist of very fine continuous pores (less than 0.08 μm in diameter), and relatively planar Ni-NiO interfaces were formed (Figures 15(a) through (c)). However, above 800 °C the Ni product microstructure consists of coarse nonuniform pore sizes, and irregular Ni-NiO interfaces were produced (Figures 15(d) through (f)). In a previous publication by the same authors,[22] the first structure was termed a *fine porous nickel-planar interfaces*, while the second structure is referred to as a *porous nickel-irregular interfaces* structure.

The result clearly demonstrates the relation between the structure of the reduction product and the reaction rate. Bearing in mind that the present data has been obtained under conditions designed to minimize the resistance due to gas film mass transfer and porous diffusion in the product layer, this indicates that the change in reaction mechanism is associated with chemical reactions occurring at the reaction interface or mass-transfer processes in the solids. Further detailed and systematic studies are required to characterize the changes in product structure and their relationship to the process conditions to enable these questions to be answered.

V. CONCLUSIONS

In the present study, the kinetics of nickel oxide reduction have been studied under controlled reaction conditions in H_2-N_2 and H_2-H_2O atmospheres. The findings of the present study are as follows.

1. Increasing hydrogen partial pressure under all conditions investigated results in an increase in rate of NiO reduction. In H_2-N_2 atmospheres, the rate is first order with respect to hydrogen partial pressure. In H_2-H_2O atmospheres, this behavior is only observed at high temperature above approximately 675 °C and steam contents below 20 pct volume H_2O.
2. In both of the H_2-N_2 and H_2-H_2O gas mixtures, it was found that the rate of formation of Ni product is not a simple monotonic function of temperature. The reaction rates were found to decrease with increasing temperatures in the range between 600 °C and 800 °C depending on the hydrogen partial pressures and reduction times.
3. There is a clear link between the rates of reduction, the nickel product morphology, and the reaction mechanisms occurring at the Ni-NiO interface.

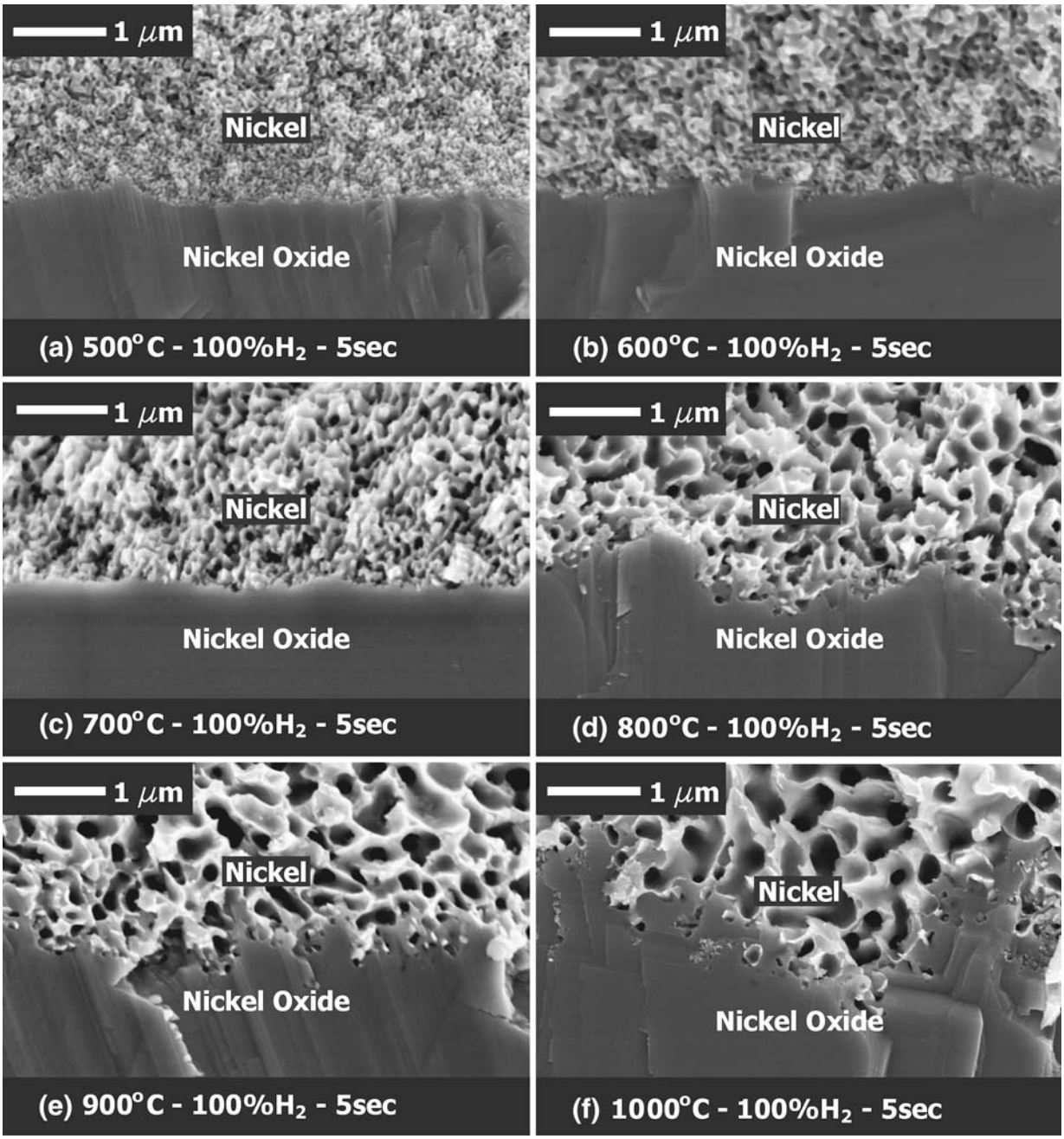

Fig. 15—Examples of interfacial structures formed during reduction of dense synthetic nickel oxide in pure H_2 (1 atm) at temperatures and times indicated.

ACKNOWLEDGMENTS

The authors thank the BHP Billiton Yabulu Refinery and Australian Research Council Linkage program for their financial support. The authors also thank AusAid for providing a scholarship for TH. The authors also acknowledge Mr. John Fittock and Dr. Joy Morgan (BHP Billiton Yabulu) for their valuable help and discussion.

REFERENCES

1. J.G. Reid and J.E. Fittock: *Int. Laterite Nickel Symp.*, Charlotte, NC, 2004, TMS, Warrendale, PA, 2004, pp. 599–618.
2. T.A. Utigard, M. Wu, G. Plascencia, and T. Marin: *Chem. Eng. Sci.*, 2005, vol. 60 (7), pp. 2061–68.
3. R.P. Furstenau, G. McDougall, and M.A. Langell: *Surf. Sci.*, 1985, vol. 150, pp. 55–79.
4. J.A. Rodriguez, J.C. Hanson, A.I. Frenkel, J.Y. Kim, and M. Perez: *J. Am. Chem. Soc.*, 2002, vol. 124 (2), pp. 346–54.

5. N.J. Themelis and W.H. Gauvin: *CIM Bull.*, 1962, vol. 55 (603), pp. 444–56.
6. C. Wagner: *Steelmaking: The Chipman Conf.*, MIT Press, Dedham, MA, 1962, pp. 19–26.
7. B.Z. Ilschner: *Metallkd.*, 1964, vol. 55, pp. 153–62.
8. K.J. Best and H.J. Grabke: *Phys.Chem.*, 1971, vol. 75, pp. 524–32.
9. K.R. Lilius: *Acta Ploytech. Scand.*, 1974, vol. 118, pp. 1–17.
10. V.V. Boldyrev, M. Bulens, and B. Delmon: *The Control of the Reactivity of Solids: Studies in Surface Science and Catalysis*, Elsevier Scientific Publishing Company, Amsterdam, 1979.
11. P.C. Hayes: *Metall. Trans. B*, 1979, vol. 10B, pp. 211–17.
12. P.C. Hayes: *Miner. Process. Extr. Metall. Rev.*, 1992, vol. 8, pp. 73–94.
13. T. Deb Roy and K.P. Abraham: *Physical Chemistry of Process Metallurgy: The Richardson Conf.*, Institute of Mining and Metallurgy, London, 1973, pp. 85–93.
14. J.W. Evans, S. Song, and C.E. Leon-Sucre: *Metall. Trans. B*, 1976, vol. 7B, pp. 55–65.
15. S. Sridhar, D. Sichen, and S. Seetharaman: *Z. Metallkd.*, 1994, vol. 85 (9), pp. 616–20.
16. A.H. Rashed and Y.K. Rao: *Chem. Eng. Commun.*, 1996, vol. 156, pp. 1–30.
17. Y.K. Rao and A.H. Rashed: *Trans. Inst. Min. Metall., Sect. C*, 2001, vol. 110, pp. 1–6.
18. S. Vogel, E. Ustundag, J.C. Hanan, V.W. Yuan, and M.A.M. Bourke: *Mater. Sci. Eng.*, 2002, vol. A333, pp. 1–9.
19. J.T. Richardson, R. Scates, and M.V. Twigg: *Appl. Catal., A*, 2003, vol. 246, pp. 137–50.
20. S.P. Matthew, D.H. St. John, J.V. Hardy, and P.C. Hayes: *Metallography*, 1985, vol. 17, pp. 367–79.
21. D.H. St. John and P.C. Hayes: *Metall. Trans. B*, 1982, vol. 13B, pp. 117–24.
22. T. Hidayat, M.A. Rhamdhani, E. Jak, and P. Hayes: *Miner. Eng.*, 2008, vol. 21 (2), pp. 157–66.
23. C.W. Bale, S.A. Degterov, G. Eriksson, K. Hack, R. Ben Mahfoud, J. Melancon, A.D. Pelton, and S. Petersen: *Calphad*, 2002, vol. 26, pp. 189–228.
24. W. Pluschkell and B.V.C. Sarma: *Arch. Eisen.*, 1974, vol. 45 (1), pp. 23–31.
25. Y. Iida and K. Shimada: *Bull. Chem. Soc. Jpn.*, 1960, vol. 33 (6), pp. 790–93.